

## Hartree-Fock-Bogoliubov nuclear mass model with 0.50 MeV accuracy based on standard forms of Skyrme and pairing functionals

S. Goriely,<sup>1</sup> N. Chamel,<sup>1</sup> and J. M. Pearson<sup>2</sup>

<sup>1</sup>*Institut d'Astronomie et d'Astrophysique, CP-226, Université Libre de Bruxelles, 1050 Brussels, Belgium*

<sup>2</sup>*Département de Physique, Université de Montréal, Montréal, Québec H3C 3J7, Canada*

(Received 6 May 2013; revised manuscript received 19 September 2013; published 5 December 2013)

We present a new Hartree-Fock-Bogoliubov nuclear mass model based on standard forms of Skyrme and pairing functionals, which corresponds to the most accurate mass model we ever achieved within the framework of the nuclear energy density functional theory. Our new mass model is characterized by a model standard deviation  $\sigma_{\text{mod}} = 0.500$  MeV with respect to essentially all the 2353 available mass data for nuclei with neutron and proton numbers larger than 8. At the same time, the underlying Skyrme functional yields a realistic description of infinite homogeneous nuclear matter properties, as determined by realistic calculations and by experiments; these include in particular the incompressibility coefficient, the pressure in charge-symmetric nuclear matter, the neutron-proton effective mass splitting, the stability against spin and spin-isospin fluctuations, as well as the neutron-matter equation of state.

DOI: [10.1103/PhysRevC.88.061302](https://doi.org/10.1103/PhysRevC.88.061302)

PACS number(s): 21.10.Dr, 21.30.-x, 21.60.Jz

Two main categories of nuclear mass model can be recognized: (i) the microscopic-macroscopic approach, based on the liquid-drop model and consisting of various degrees of refinement of the original Weizsäcker mass model [1], e.g., the new finite-range drop model of Möller *et al.* [2] and the work of Liu *et al.* [3]; (ii) the Hartree-Fock-Bogoliubov (HFB) approach followed by our group, using density functionals based on Skyrme-type or Gogny-type effective interactions; the most recent versions are found in Refs. [4–6].

Despite the great differences between these two approaches they can both be said to be “semi-empirical” in the sense that they contain a certain number of parameters that are determined by fitting to essentially all the available mass data. The presence of such free parameters is made necessary by the hitherto very limited success of *ab initio* approaches, in which one tries to derive nuclear masses, along with all other nuclear properties, from the “real” basic interactions between nucleons, as determined by the properties of two- and three-nucleon systems. So far this approach has succeeded only for nuclei with mass number  $A \leq 74$  (see, for example, Ref. [7]) and homogeneous or infinite nuclear matter (INM).

Insofar as the interest of mass models lies in the calculation of masses of nuclei that cannot be measured at the present time, the presence of parameters that are fitted to the mass data inevitably raises questions as to the reliability of such extrapolations. Indeed, for this reason in our own work [4–6] we require that some of our parameters satisfy constraints derived from *ab initio* calculations of INM. Actually, a number of groups [8–10] have calculated nuclear masses with methods that are much closer in spirit to the *ab initio* approach than are either of the first two categories that we have mentioned. However, very heavy computation is required, and so far such functionals have not been able to reproduce existing nuclear data with the same degree of accuracy as more phenomenological methods. Thus these promising methods cannot yet be said to have led to viable mass models.

Our concern in this paper is with our own Skyrme-HFB approach. In two recent papers [5,6] we have presented a

family of eight Skyrme-type functionals, BSk19 to BSk26, along with their corresponding mass tables, HFB-19 to HFB-26, respectively, that we constructed with a view to providing a unified approach not only to the structure of all the different regions of neutron stars (outer crust, inner crust, and core) but also to other phenomena associated with the birth and death of neutron stars, such as supernova core collapse, the *r* process of nucleosynthesis (both in the neutrino-driven wind and during the decompression of neutron-star matter). These functionals are all based on effective forces with a 16-parameter generalized Skyrme form, characterized by unconventional terms that have simultaneous density and momentum dependence.

The parameters of this form of force were determined primarily by fitting measured nuclear masses, which were calculated with the HFB method. For this it was necessary to supplement the Skyrme forces with a pairing force, phenomenological Wigner terms, and correction terms for the spurious collective energy. However, in fitting the mass data we simultaneously constrained the Skyrme force to fit the zero-temperature equation of state (EoS) of homogeneous neutron matter (NeuM), as determined by many-body calculations with realistic two- and three-nucleon forces.

Actually, a wide range of EoSs of NeuM have been proposed, differing greatly in the predicted stiffness at the densities encountered in neutron star cores, but the form of our functionals is sufficiently flexible to allow each of them to be fitted, with an appropriate choice of parameters, while at the same time obtaining a precise fit to the mass data. Our preferred functional, BSk24 (mass model HFB-24) [6], fits the 2353 measured masses of nuclei with  $N$  and  $Z \geq 8$  appearing in the 2012 Atomic Mass Evaluation [11] with an rms deviation of 0.549 MeV, and supports the heaviest observed neutron stars.

Moreover, our functionals simultaneously achieved (a) a precise fit to the charge-radius data [12] (in the case of BSk24 the rms deviation is 0.026 fm) as well as a good description of the charge density radial distribution; (b) a value of  $0.8M$  for the isoscalar effective mass  $M_s^*$  in

charge-symmetric INM at the appropriate equilibrium density  $n_0$ , this being the value indicated by calculations on INM with realistic forces (see the discussion in Ref. [13]); (c) an incompressibility  $K_v$  of charge-symmetric INM falling in the experimental range  $240 \pm 10$  MeV [14]; (d) the stability of NeuM and of  $\beta$ -equilibrated neutron star matter (i.e., the homogeneous nucleon-lepton mixture of which neutron star cores are comprised) against an unphysical polarization at any density relevant to neutron star cores [15,16]; (e) an EoS of charge-symmetric INM that is consistent with measurements in heavy-ion collisions of nuclear-matter flow over the density range  $3-4.5n_0$  [17,18]; and (f) a qualitatively acceptable distribution of potential energy among the four different spin-isospin channels in INM.

However, this success was possible only because of the presence of the unconventional  $t_4$  and  $t_5$  terms in the Skyrme force, which introduce considerable complexity into the formalism (see the Appendix of Ref. [15]). Furthermore, while the usual  $\delta$ -function form of pairing force was taken, our treatment of its density dependence was far from conventional: Rather than postulating a simple functional form for the density dependence, the pairing strength was calculated analytically at each point in the nucleus in question in such a way as to reproduce the  $^1S_0$  pairing gaps of INM of the appropriate density and charge asymmetry, as determined by many-body calculations with realistic two- and three-nucleon forces [19–21].

Realizing that our unconventional functionals cannot be used in many nuclear structure codes, we explore in the present paper the extent to which it is possible to reproduce the successes of functional BSk24 with a standard form of functional, i.e., using a 10-parameter Skyrme force of the form

$$\begin{aligned}
v_{ij} = & t_0(1 + x_0 P_\sigma) \delta(\mathbf{r}_{ij}) + t_1(1 + x_1 P_\sigma) \frac{1}{2\hbar^2} \{ p_{ij}^2 \delta(\mathbf{r}_{ij}) \\
& + \delta(\mathbf{r}_{ij}) p_{ij}^2 \} + t_2(1 + x_2 P_\sigma) \frac{1}{\hbar^2} \mathbf{p}_{ij} \cdot \delta(\mathbf{r}_{ij}) \mathbf{p}_{ij} \\
& + \frac{1}{6} t_3(1 + x_3 P_\sigma) n(\mathbf{r})^\gamma \delta(\mathbf{r}_{ij}) \\
& + \frac{i}{\hbar^2} W_0 (\boldsymbol{\sigma}_i + \boldsymbol{\sigma}_j) \cdot \mathbf{p}_{ij} \times \delta(\mathbf{r}_{ij}) \mathbf{p}_{ij}, \quad (1)
\end{aligned}$$

and a pairing force of the form

$$v_{\text{pair}}(\mathbf{r}_{ij}) = V_{\pi q} \left[ 1 - \eta \left( \frac{n}{n_0} \right)^\alpha \right] \delta(\mathbf{r}_{ij}), \quad (2)$$

where  $\mathbf{r}_{ij} = \mathbf{r}_i - \mathbf{r}_j$ ,  $\mathbf{r} = (\mathbf{r}_i + \mathbf{r}_j)/2$ ,  $\mathbf{p}_{ij} = -i\hbar(\nabla_i - \nabla_j)/2$  (this is the relative momentum),  $P_\sigma$  is the two-body spin-exchange operator, and  $n(\mathbf{r})$  is the total local density.

As in our previous mass models [5,6,15,19,20], the above mentioned constraints are again applied. We also impose a symmetry coefficient  $J = 30$  MeV, which was shown to provide a good description of the NeuM EoS at low densities and of nuclear masses and neutron skin data of nuclei [6]. In particular, it was shown in Ref. [6] that an increase of  $J$  by 1 or 2 MeV leads to an increase of the rms deviation by typically 20 and 80 keV, respectively. Similar results were found in our previous mass fits based on standard Skyrme functionals [22]. In addition, all the terms quadratic in the

TABLE I. Parameters of the HFB-27\* mass model: first two columns shows the parameters of the underlying Skyrme force BSk27\*, third and fourth columns the pairing parameters and last two columns the parameters for the Wigner and collective corrections (units for energy and length are MeV and fm, respectively).

Parameter	Value	Parameter	Value	Parameter	Value
$t_0$	-1837.06	$V_{\pi n}^+$	-456.6	$V_W$	-2.40
$t_1$	376.186	$V_{\pi n}^-$	-482.1	$\lambda$	230
$t_2$	-60.3080	$V_{\pi p}^+$	-500.2	$V'_W$	1.08
$t_3$	11521.7	$V_{\pi p}^-$	-527.6	$A_0$	25
$x_0$	0.460067	$\varepsilon_\Lambda$	16.0	$b$	0.8
$x_1$	-0.385853			$c$	10
$x_2$	1.25982			$d$	3.7
$x_3$	0.640301			$l$	16
$W_0$	114.631			$\beta_2^0$	0.1
$\gamma$	0.3				

spin-current tensor and their time-odd counterpart are dropped from the functional; as discussed in Ref. [5,16], this ansatz (i) leads to more realistic values for the Landau parameters and the Landau sum rules and (ii) removes spurious spin and spin-isospin instabilities in nuclear matter, including in particular unphysical ferromagnetic transitions over the full range of densities relevant to neutron stars. Finally, we drop the Coulomb exchange term for protons. This is a device that leads to a significant improvement in the mass fits, especially mirror-nucleus differences, and it can be interpreted as simulating neglected effects such as Coulomb correlations, charge-symmetry breaking of the nuclear forces, and vacuum polarization [23]. For the pairing force, we use the same parameters  $\eta = 0.45$  and  $\alpha = 0.47$  as found in Ref. [24] and include only single-particle states of energy  $\pm\varepsilon_\Lambda$  around the Fermi level (Table I). In an attempt to take into account Coulomb and charge-symmetry-breaking effects, as well as time-reversal effects, the strength parameter  $V_{\pi q}$  was allowed to be different for neutrons and protons, and also to be slightly stronger for an odd number of nucleons ( $V_{\pi q}^-$ ) than for an even number ( $V_{\pi q}^+$ ); i.e., the pairing force between neutrons, for example, depends on whether the neutron number  $N$  is even or odd.

To go beyond the mean-field approach, we subtract from the HFB energy an estimate for the spurious collective energy. As described in Ref. [19], the form we adopt here (and in Refs. [5,6]) is

$$E_{\text{coll}} = E_{\text{rot}}^{\text{crank}} \{ b \tanh(c|\beta_2|) + d|\beta_2| e^{-l(|\beta_2| - \beta_2^0)^2} \} \quad (3)$$

in which  $E_{\text{rot}}^{\text{crank}}$  denotes the cranking-model value of the rotational correction and  $\beta_2$  denotes the quadrupole deformation, while all other parameters are fitted freely. While the first term here represents the rotational correction, phenomenologically modified from its cranking-model value, the second term takes account of the deformation dependence of the vibrational correction (since  $E_{\text{coll}}$  as given by Eq. (3) vanishes for spherical nuclei we suppose that the vibrational correction for such nuclei is absorbed into the fitted force parameters). The latter correction has been shown to be of prime importance for a proper description of shape isomers and fission barriers [25].

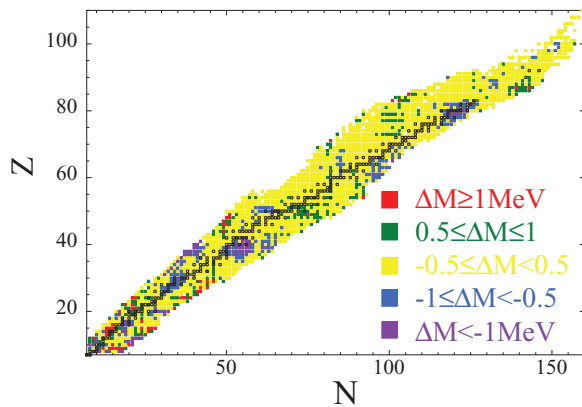


FIG. 1. (Color online) Representation in the  $(N, Z)$  plane of the difference between measured [11] and HFB-27\* masses. Open squares represent stable (including the long-lived Th and U isotopes) nuclei.

To describe the well-known overbinding found in the  $N \simeq Z$  nuclei, the final mass formula adds to the above-described energy a phenomenological Wigner term of the form

$$E_W = V_W e^{-\lambda((N-Z)/A)^2} + V'_W |N - Z| e^{-(A/A_0)^2} \quad (4)$$

which contributes significantly only for light nuclei ( $A < A_0$ ) or nuclei with  $N \sim Z$ . Our treatment of this correction is purely phenomenological, although physical interpretations of each of the two terms can be made [19,26].

*Results.* The foregoing model, labeled HFB-27\* (we now adopt the notation \* to refer to results obtained with standard Skyrme functionals), was fitted to the full data set of 2353 measured nuclear masses [11]; the resulting parameter set, labeled BSk27\*, is given in Table I. We plot in Fig. 1 the difference  $M_{\text{exp}} - M_{\text{th}}$  for all the 2353 nuclei with  $Z$  and  $N \geq 8$  for which the mass is known; no deviation exceeds 2.5 MeV. The rms and mean values of these deviations are shown in the first two lines of Table II, with an rms deviation of 0.512 MeV, which is lower than achieved in any of our previous models. Table II also gives the deviation for the subset of 257 masses of neutron-rich nuclei with  $S_n \leq 5$  MeV, the neutron separation energies ( $S_n$ ) and the  $\beta$ -decay  $Q$  values. Because experimental errors can give a significant contribution to the rms deviation we also give in Table II the model error ( $\sigma_{\text{mod}}$ ) as defined by Eqs. (42) and (43) of Ref. [27]. As can be seen in Table II, the model error for HFB-27\* has now reached the value of 0.500 MeV.

Even though the BSk27\* functional was primarily fitted to nuclear masses, it also provides a realistic description of INM. Table III shows the corresponding macroscopic parameters. For comparison, we have also indicated the values of these parameters for the generalized Skyrme functional BSk24 [6]. Note that in both cases, the same values of the isoscalar effective mass  $M_s^*$  and symmetry energy  $J$  were imposed. For both forces, the isovector effective mass  $M_v^*$  is found to be smaller than  $M_s^*$  at the saturation density  $n_0$ , implying that the neutron effective mass  $M_n^*$  is larger than the proton effective mass  $M_p^*$  in neutron-rich matter. Such an isovector splitting of the effective mass is consistent with measurements of isovector giant resonances [28] and has been confirmed in

TABLE II. Rms ( $\sigma$ ) and mean ( $\bar{\epsilon}$ ) deviations between data and predictions for the HFB-27\* model of this paper. The first pair of lines refers to all the 2353 measured masses that were fitted [11], the third line to the corresponding model error, the next pair to the masses  $M_{nr}$  of the subset of 257 neutron-rich nuclei with  $S_n \leq 5.0$  MeV, and the following two pairs to the 2199  $S_n$  and 2065  $Q_\beta$  measured values. The last pair corresponds to charge radii (884 measured values [12]). For comparison, the results obtained with the HFB-24 mass model [6] are also given.

	HFB-24	HFB-27*
$\sigma(M)$ (MeV)	0.549	0.512
$\bar{\epsilon}(M)$ (MeV)	-0.012	-0.005
$\sigma_{\text{mod}}(M)$ (MeV)	0.542	0.500
$\sigma(M_{nr})$ (MeV)	0.702	0.645
$\bar{\epsilon}(M_{nr})$ (MeV)	0.011	0.051
$\sigma(S_n)$ (MeV)	0.474	0.425
$\bar{\epsilon}(S_n)$ (MeV)	-0.009	-0.003
$\sigma(Q_\beta)$ (MeV)	0.567	0.516
$\bar{\epsilon}(Q_\beta)$ (MeV)	0.010	0.002
$\sigma(R_c)$ (fm)	0.026	0.028
$\bar{\epsilon}(R_c)$ (fm)	-0.001	0.010

several many-body calculations with realistic forces [29,30]. It is quite remarkable that the actual values of the effective masses predicted by both forces are in close agreement with those obtained in Ref. [8], namely  $M_s^* = 0.825M$  and  $M_v^* = 0.727M$ . It is to be noted that unlike in Ref. [28], we have not had to resort to a second  $t_3$  term in the Skyrme force in order to obtain the correct sign for the isovector splitting of the nucleon effective mass while fitting a realistic NeuM EoS. As shown in Fig. 2, the charge-symmetric INM EoS as obtained from our functional BSk27\* is consistent with the analysis of the matter flow in heavy-ion collision experiments at densities ranging from  $\sim n_0$  to  $\sim 4.5n_0$  [17,18].

As shown in Fig. 3, the NeuM EoSs predicted by BSk27\* and BSk24 are both compatible with recent quantum Monte Carlo calculations [31] up to a density of about  $0.5 \text{ fm}^{-3}$  at least, but also with those obtained by Tews *et al.* [32] at next-to-next-to-next-to-leading order in chiral effective field

TABLE III. Macroscopic parameters for forces BSk24 and BSk27\*. Note that units for energy and length are MeV and fm, respectively. For the definition of the parameters, see, for example, Ref. [19].

	BSk24	BSk27*
$a_v$	-16.048	-16.051
$n_0$	0.1578	0.1586
$J$	30.0	30.0
$M_s^*/M$	0.80	0.80
$M_v^*/M$	0.71	0.72
$K_v$	245.5	241.6
$K_{\text{sym}}$	-37.6	-221.4
$K'$	274.5	363.5
$L$	46.40	28.5
$G_0$	0.57	0.59
$G'_0$	0.95	0.95

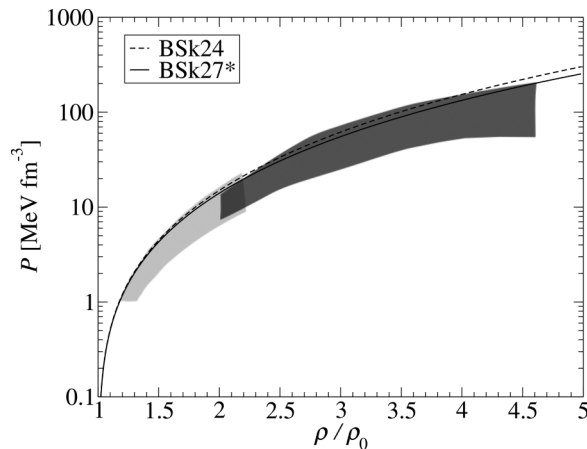


FIG. 2. Pressure as a function of density in charge-symmetric nuclear matter for the Skyrme functional BSk24 [6] and for our new Skyrme functional BSk27\*. The shaded area represents the constraint inferred from the analysis of heavy-ion collisions [17,18].

theory. On the other hand, the high-density stiffness of these two NeuM EoSs differs significantly: BSk24 is the stiffest possible, while BSk27\* is the softest with respect to the constraints shown in Fig. 3. If extrapolated to the high densities prevailing in neutron star cores, the very soft NeuM predicted by the BSk27\* functional appears to be ruled out by the measured mass of PSR J1614–2230 [33]. We were unable to get a stiffer NeuM EoS without degrading the quality of the mass fit or including additional terms that are simultaneously density and momentum dependent, as done in Refs. [5,6]. In this respect, generalized Skyrme functionals, like BSk24, seem better suited for applications to neutron star cores. On the other hand, massive neutron stars are not necessarily incompatible with a soft nucleonic EoS: It may suffice that neutron-star cores contain non-nucleonic matter (e.g., deconfined quarks) with a sufficiently stiff EoS, as discussed, e.g., in Ref. [34]. As a matter of fact, a soft nucleonic EoS is suggested by the

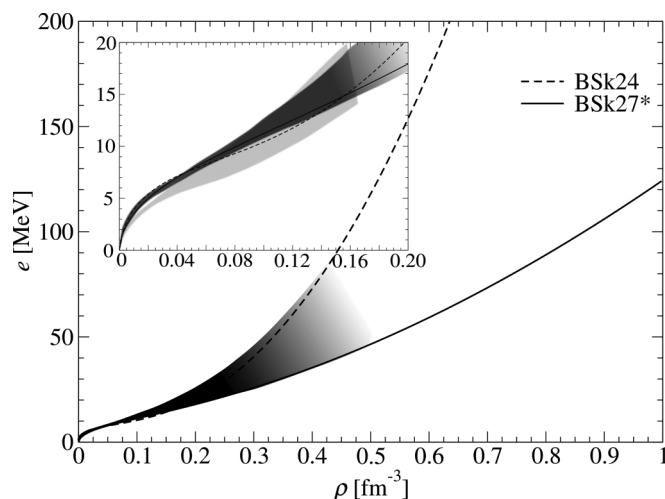


FIG. 3. Zero-temperature equation of state of neutron matter as obtained with the Skyrme functional BSk24 [6] and with our new Skyrme functional BSk27\*. The shaded areas represent the recent constraints of Ref. [31] (dark) and of Ref. [32] (light).

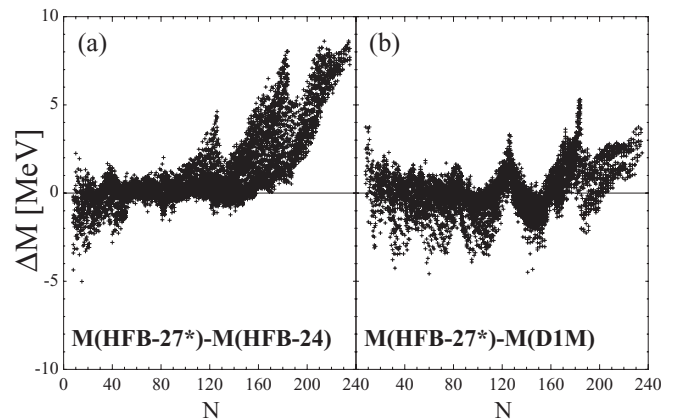


FIG. 4. Differences between (a) HFB-27\* and HFB-24 [6] masses and (b) HFB-27\* and D1M [4] masses for all  $Z, N \geq 8, Z \leq 110$  nuclei between the proton and neutron drip lines.

analysis of  $K^+$  production [35–37] and  $\pi^-/\pi^+$  production ratio [38] that have been measured in heavy-ion collisions.

Unlike our previous nuclear mass models since HFB-16 [19], the pairing force that we have adopted here is purely phenomenological. It has been already shown that the density dependence given by Eq. (2) is not flexible enough to allow for a good fit of the  $^1S_0$  pairing gaps in both charge-symmetric INM and NeuM, as obtained from microscopic calculations using realistic nucleon-nucleon potentials [21,39,40]. This is clearly a deficiency of the standard pairing force given by Eq. (2). For this reason, the pairing functionals underlying our previous mass models from HFB-16 to HFB-26, which were all deduced from microscopic calculations [21], are much better suited for studies of superfluidity in neutron star crusts than the pairing functional underlying the HFB-27\* mass model.

We have constructed a complete mass table including all nuclei in the range  $Z$  and  $N \geq 8$  and  $Z \leq 110$  located between the proton and neutron-drip lines. In Fig. 4, we compare these predictions with those of our mass model HFB-24 and the Gogny-HFB mass calculation based on the D1M force [4]. When comparing with our new mass model, we see that relatively small differences emerge, except for the heaviest nuclei ( $Z > 80$ ) and as the neutron-drip line is approached ( $N > 160$ ). Even smaller deviations are found with respect to the D1M mass model, except in the vicinity of the  $N = 126$  or 184 neutron shell closures.

*Conclusions.* We have shown that with standard forms of Skyrme and pairing forces it is possible to get an even better fit to the mass data than was possible with the BSk24 functional, the rms deviation for the 2353 measured masses of nuclei with  $N$  and  $Z \geq 8$  having been reduced to 0.512 MeV and the model deviation to 0.500 MeV. However, to do this we had to drop the requirement of an EoS of NeuM stiff enough to support the heaviest neutron stars that have been observed. (It could be that the necessary support comes from non-nucleonic matter such as hyperons and quarks, but this is far from clear at the present time, while the generalized form of functional adopted in Refs. [5,6] is flexible enough to support the heaviest neutron stars without invoking non-nucleonic matter.)



Nevertheless, the new functional fits the EoS of NeuM up to densities of  $3-4n_0$ . Moreover, other nuclear-matter properties, such as the incompressibility coefficient, the isoscalar and isovector effective masses, the pressure in charge-symmetric INM, and stability against spin and spin-isospin fluctuations are predicted to have values consistent with both experiments and calculations based on realistic nucleon-nucleon potentials.

Thus we believe that the new functional will have widespread applicability in standard HFB codes, although for unified treatments of all parts of neutron stars a generalized functional such as BSk24 will still be necessary.

*Acknowledgments.* S.G. and N.C. acknowledge financial support from FNRS (Belgium), and J.M.P. acknowledges funding from NSERC (Canada).

- 
- [1] C. F. von Weizsäcker, *Z. Phys.* **96**, 431 (1935).  
 [2] P. Möller, W. D. Myers, H. Sagawa, and S. Yoshida, *Phys. Rev. Lett.* **108**, 052501 (2012).  
 [3] M. Liu, N. Wang, Y. Deng, and X. Wu, *Phys. Rev. C* **84**, 014333 (2011).  
 [4] S. Goriely, S. Hilaire, M. Girod, and S. Péru, *Phys. Rev. Lett.* **102**, 242501 (2009).  
 [5] S. Goriely, N. Chamel, and J. M. Pearson, *Phys. Rev. C* **82**, 035804 (2010).  
 [6] S. Goriely, N. Chamel, and J. M. Pearson, *Phys. Rev. C* **88**, 024308 (2013).  
 [7] V. Somà, C. Barbieri, and T. Duguet, *Phys. Rev. C* **87**, 011303(R) (2013).  
 [8] L. G. Cao, U. Lombardo, C. W. Shen, and N. V. Giai, *Phys. Rev. C* **73**, 014313 (2006).  
 [9] D. Gambacurta, L. Li, G. Colò, U. Lombardo, N. Van Giai, and W. Zuo, *Phys. Rev. C* **84**, 024301 (2011).  
 [10] J. Erler, C. J. Horowitz, W. Nazarewicz, M. Rafalski, and P.-G. Reinhard, *Phys. Rev. C* **87**, 044320 (2013).  
 [11] G. Audi, M. Wang, A. H. Wapstra, F. G. Kondev, M. MacCormick, X. Xu, and B. Pfeiffer, *Chin. Phys. C* **36**, 1287 (2012).  
 [12] I. Angeli and K. P. Marinova, *At. Data Nucl. Data Tables* **99**, 69 (2013).  
 [13] S. Goriely, M. Samyn, M. Bender, and J. M. Pearson, *Phys. Rev. C* **68**, 054325 (2003).  
 [14] G. Colò, N. V. Giai, J. Meyer, K. Bennaceur, and P. Bonche, *Phys. Rev. C* **70**, 024307 (2004).  
 [15] N. Chamel, S. Goriely, and J. M. Pearson, *Phys. Rev. C* **80**, 065804 (2009).  
 [16] N. Chamel and S. Goriely, *Phys. Rev. C* **82**, 045804 (2010).  
 [17] P. Danielewicz, R. Lacey, and W. G. Lynch, *Science* **298**, 1592 (2002).  
 [18] Lynch *et al.*, *Prog. Part. Nucl. Phys.* **62**, 427 (2009).  
 [19] N. Chamel, S. Goriely, and J. M. Pearson, *Nucl. Phys. A* **812**, 72 (2008).  
 [20] S. Goriely, N. Chamel, and J. M. Pearson, *Phys. Rev. Lett.* **102**, 152503 (2009).  
 [21] N. Chamel, *Phys. Rev. C* **82**, 014313 (2010).  
 [22] S. Goriely, M. Samyn, J. M. Pearson, and M. Onsi, *Nucl. Phys. A* **750**, 425 (2005).  
 [23] S. Goriely and J. M. Pearson, *Phys. Rev. C* **77**, 031301(R) (2008).  
 [24] E. Garrido, P. Sarriguren, E. Moya de Guerra, and P. Schuck, *Phys. Rev. C* **60**, 064312 (1999).  
 [25] S. Goriely, M. Samyn, and J. M. Pearson, *Phys. Rev. C* **75**, 064312 (2007).  
 [26] S. Goriely, M. Samyn, P.-H. Heenen, J. M. Pearson, and F. Tondeur, *Phys. Rev. C* **66**, 024326 (2002).  
 [27] P. Möller and J. R. Nix, *At. Data Nucl. Data Tables* **39**, 213 (1988).  
 [28] T. Lesinski, K. Bennaceur, T. Duguet, and J. Meyer, *Phys. Rev. C* **74**, 044315 (2006).  
 [29] E. N. E. van Dalen, C. Fuchs, and A. Faessler, *Phys. Rev. Lett.* **95**, 022302 (2005).  
 [30] W. Zuo, U. Lombardo, H.-J. Schulze, and Z. H. Li, *Phys. Rev. C* **74**, 014317 (2006).  
 [31] S. Gandolfi, J. Carlson, and S. Reddy, *Phys. Rev. C* **85**, 032801 (R) (2012).  
 [32] I. Tews, T. Krüger, K. Hebeler, and A. Schwenk, *Phys. Rev. Lett.* **110**, 032504 (2013).  
 [33] P. B. Demorest, T. Pennucci, S. M. Ransom, M. S. E. Roberts, and J. W. T. Hessels, *Nature (London)* **467**, 1081 (2010).  
 [34] N. Chamel, A. F. Fantina, J. M. Pearson, and S. Goriely, *Astron. Astrophys.* **553**, A22 (2013).  
 [35] C. Fuchs, A. Faessler, E. Zabrodin, and Y.-M. Zheng, *Phys. Rev. Lett.* **86**, 1974 (2001).  
 [36] C. Sturm, I. Böttcher, M. Dzebovski *et al.*, *Phys. Rev. Lett.* **86**, 39 (2001).  
 [37] C. Hartnack, H. Oeschler, and J. Aichelin, *Phys. Rev. Lett.* **96**, 012302 (2006).  
 [38] Z. Xiao, B.-A. Li, L.-W. Chen, G.-C. Yong, and M. Zhang, *Phys. Rev. Lett.* **102**, 062502 (2009).  
 [39] S. S. Zhang, L. G. Cao, U. Lombardo, E. G. Zhao, and S. G. Zhou, *Phys. Rev. C* **81**, 044313 (2010).  
 [40] J. Margueron, H. Sagawa, and K. Hagino, *Phys. Rev. C* **77**, 054309 (2008).